JPET Fast Forward. Published on April 21, 2005 as DOI: 10.1124/jpet.105.086504

Variability of CYP3A7 Expression in Human Fetal Liver

J. Steven Leeder, Roger Gaedigk, Kenda A. Marcucci, Andrea Gaedigk, Carrie A. Vyhlidal,

Bradley P. Schindel and Robin E. Pearce

Section of Developmental Pharmacology and Experimental Therapeutics (JSL, RG, KAM, AG, CAV, BPS, REP), Division of Pediatric Pharmacology and Medical Toxicology, Department of Pediatrics, Children's Mercy Hospital and Clinics, Kansas City, MO 64108

Running Title: Variability of CYP3A7 Expression in Human Fetal Liver

Corresponding Author:

J Steven Leeder

Section of Developmental Pharmacology and Experimental Therapeutics

Children's Mercy Hospital and Clinics

2401 Gillham Road

Kansas City, MO 64108

Phone: (816) 234-3059

Fax: (816) 855-1958

Email: sleeder@cmh.edu

Number of text pages: 23

Number of tables: 5

Number of figures: 5

Number of references: 32

Number of words in the *Abstract*: 242

Number of words in the *Introduction*: 625

Number of words in the *Discussion*: 1454

List of non-standard abbreviations:

DHEA, dehydroepiandrosterone; DHEA-S, dehydroepiandrosterone 3-sulfate; 16αDHEA, 16α-hydroxy DHEA; DHEA16αH, dehydroepiandrosterone 16α-hydroxylation; PMI, post mortem interval; QRT-PCR, quantitative reverse transcriptase polymerase chain reaction; T2αH, testosterone 2α-hydroxylation; T6βH, testosterone 6β-hydroxylation

JPET Fast Forward. Published on April 21, 2005 as DOI: 10.1124/jpet.105.086504
This article has not been copyedited and formatted. The final version may differ from this version.

Abstract

Fetal liver CYP3A7 plays an important role in placental estriol synthesis during pregnancy, yet little is known concerning the extent or consequences of variability in expression. The purpose of this investigation was to characterize the variability in CYP3A7 expression using several phenotypic measures in a panel of 54 fetal livers ranging in age from 76 d to 32 wk gestation. CYP3A7 mRNA expression was measured using quantitative PCR while immunoreactive CYP3A7 was determined using an affinity-purified anti-peptide antibody. Variability in catalytic activity was evaluated using testosterone and dehydroepiandrosterone (DHEA) as substrates. Across the entire panel, CYP3A7 was the most abundant CYP3A mRNA species present and varied 634-fold from 151 to 95700 transcripts/ng total RNA, corrected for 18S ribosomal RNA. CYP3A4 expression was minimal based on mRNA expression (1,000-fold lower than CYP3A7) and the ratio of testosterone 2α- (T2αH) to 6β- (T6βH) hydroxylation. T2αH and T6βH were highly correlated (r^2=0.859) and the correlation increased (r^2=0.974) in livers with *CYP3A5*3/*3* genotypes implying that the same enzyme (CYP3A7) generated both products. Overall, T2αH and DHEA16αH activities varied 175- and 250-fold, respectively. A subset of five samples had extremely low mRNA, protein and catalytic activity, possibly due to pathology affecting fetal viability (anencephaly, porencephaly). In the remaining samples, T2αH activity varied 6.7-fold (358±142, range 97 to 643 pmol/min/mg) and DHEA16αH activity varied 6.2-fold (8.07±2.87, range 2.41 to 14.9 nmol/min/mg). Observed variability in CYP3A7 activity was not related to *CYP3A7*2,* and alternative regulatory mechanisms require further investigation.

JPET Fast Forward. Published on April 21, 2005 as DOI: 10.1124/jpet.105.086504
This article has not been copyedited and formatted. The final version may differ from this version.

Introduction

Approximately 10 years ago, Nebert proposed that drug biotransformation is but a small component of a much broader set of functions that can be ascribed to "effector ligand-metabolizing enzymes" (Nebert, 1991; Nebert, 1994). The central tenet of this thesis is that small (<500 Da) endogenous ligands involved in growth and differentiation (*e.g.* androgens, cholesterol, eicosanoids, estrogens, progestins, retinoic acid, thyroxine, and vitamin D, among others) are subject to oxidative metabolism and conjugation by the same pathways responsible for xenobiotic detoxification. Furthermore, it is quite clear that fetal development involves the coordinated actions of complex networks of genes that interact during organogenesis, as receptor systems and signal transduction networks become established, and as organ function matures in preparation for perinatal survival.

For over 40 years, estriol has been recognized as the "pregnancy estrogen". It is an important determinant of fetal growth and development as well as timing of parturition (Mesiano and Jaffe, 1997), and its biosynthetic pathway exemplifies a network of "effector ligand-metabolizing enzymes". For example, SULT2A1 is responsible for dehydroepiandrosterone 3-sulfate (DHEA-S) synthesis in the fetal adrenal, and the majority of DHEA-S subsequently undergoes 16α-hydroxylation in the fetal liver (and, to a lesser extent, within the adrenal itself (Serón-Ferré and Jaffe, 1981)), an activity that has been attributed to CYP3A7 (Kitada et al., 1987). After uptake into placental syncytiotrophoblasts, DHEA-S and 16α-hydroxydehydroepiandrosterone 3-sulfate (16αDHEA-S) are deconjugated by sulfatase to generate DHEA and 16αDHEA, the primary C_{19} steroid precursors for aromatase (CYP19)-mediated estradiol and estriol synthesis, respectively (Ryan, 1959; Baulieu and Dray, 1963; Siiteri and MacDonald, 1963).

CYP3A7 would appear to have important functions in addition to its role in estriol biosynthesis. Catalytic activity attributed to CYP3A7 has been observed in embryonic liver as early as 50-60 days gestation (Yang et al., 1994). Expression has been reported to increase throughout pregnancy, peaking at two weeks postnatal age (PNA) and declining thereafter to the low levels characteristic of adult liver (Lacroix et al., 1997) although more recent data suggest that activity declines throughout the last trimester of pregnancy (Stevens et al., 2003). Nevertheless, DHEA-S in high concentrations is associated with inhibition of cell proliferation and progesterone synthesis, leading to speculation that functional DHEA-S 16α-hydroxylation may also play a fetoprotective function (Schuetz et al., 1993). Consistent with this hypothesis, DHEA-S and other 3-conjugated steroids have been reported to activate the catalytic activity of CYP3A7, but not CYP3A4 (Nakamura et al., 2003). Furthermore, given its catalytic activity towards the 4-hydroxylation of 9-*cis* and all-*trans*-retinoic acid (Chen et al., 2000; Marill et al., 2000; Marill et al., 2002), CYP3A7 may also provide protection against the embryotoxic effects of retinoic acid, particularly from exogenous exposure following maternal ingestion of therapeutic doses. Finally, it appears that CYP3A7 also possesses the capacity to bioactivate several promutagens, including aflatoxin B_1 (Li et al., 1997).

Given these considerations and the fact that the extent of inter-individual variation in fetal liver CYP3A7 activity is essentially unknown, the purpose of this investigation was to characterize the extent of variability in CYP3A7 mRNA transcripts, protein expression and catalytic activity towards endogenous and xenobiotic substrates in a panel of fetal liver tissues. Since the DHEA 16α-hydroxylation activities reported by Stevens *et al.* (Stevens et al., 2003) were approximately 10-fold higher than those reported by Lacroix *et al.* (Lacroix et al., 1997), estimates of catalytic activity and expression levels of mRNA are critically dependent upon tissue quality.

Furthermore, difficulty in discriminating between CYP3A4 and CYP3A7 activities and immunoreactive protein content has been a historical problem when using conventional probes of CYP3A activity and commercially available antibodies (Stevens et al., 2003). To address these issues, the current investigation implemented strict tissue selection criteria and utilized a variety of experimental approaches to unambiguously differentiate CYP3A7-related activity from that of CYP3A4 or CYP3A5.

Methods

Materials and Reagents. Testosterone, androstenedione, 2α-hydroxytestosterone, 2β-hydroxytestosterone, 6β-hydroxytestosterone, 15α-hydroxytestosterone, glucose-6-phospate, glucose-6-phosphate dehydrogenase, NADP and EDTA were purchased from Sigma-Aldrich Co. (St. Louis, MO). Dehydroepiandrosterone (DHEA) and 16α-hydroxydehydroepiandrosterone (16αDHEA) were purchased from Steraloids (Newport, RI). All other reagents were of analytical grade. Microsomes prepared from baculovirus-infected insect cells (SUPERSOMES) expressing human P450 enzymes CYPs 1A1, 1A2, 1B1, 2A6, 2B6, 2C8, 2C9, 2C18, 2C19, 2D6, 2E1, 3A4, 3A5, 3A7 or control vector were purchased from BD Gentest (Woburn, MA). Criterion 4-15% Tris-HCl gels and Tris/Glycine/SDS running buffer were purchased from BioRad (Hercules, CA). Hybond C-Super nitrocellulose, ECL Anti-rabbit IgG HRP conjugated antibody, ECL Plus Detection Kit, and Hyperfilm were purchased from Amersham Biosciences (Piscataway, NJ).

Liver Samples. A total of 54 liver samples 76 d to 32 wk estimated gestational age (EGA) were obtained through NICHD-supported tissue retrieval programs, 26 from the Central Laboratory for Human Embryology at the University of Washington (Seattle, WA) and 28 from the Brain and Tissue Bank for Developmental Disorders at the University of Maryland (Baltimore, MD). Available demographic data are presented in Table 1. Tissues were stored at -70º C prior to preparation of subcellular fractions. The post mortem interval was 2 h or less for 49 samples; five had post mortem intervals of 3 h (n=2), 4 h (n=1), 5 h (n=1) and 6 h (n=1). The use of these tissues was approved by the University of Missouri-Kansas City Pediatric Health Sciences Review Board.

Preparation of Fetal Liver Microsomes. Microsomes were prepared from 51 of the 54 human fetal livers by differential centrifugation according to the method of Lu and Levin (Lu and Levin, 1972). Isolated microsomal pellets were removed from centrifuge tubes with a Teflon-coated spatula, transferred to a low-volume glass mortars (tapered, 4 ml), manually resuspended in 0.25 M sucrose with a tapered, Teflon pestle and stored at -70ºC until use. Protein concentrations were determined using the Micro BCA Protein Assay kit (Pierce Chemical Co., Rockford, IL).

RNA Extraction and Quantitative Real Time (QRT)-PCR Analysis. Frozen liver tissues (20 mg to 30 mg) were homogenized and total RNA extracted according to the Qiagen RNeasy protocol (Qiagen, Valencia, CA) with an on-column DNase I treatment. The quality of the isolated RNA was assessed by agarose gel electrophoresis, and RNA quantity was determined spectrophotometrically. For one step QRT-PCR reactions, RNA was diluted to 5 ng/µl and 25 ng were used in a reaction volume of 20 µl. Primer pairs designed to specifically bind in exon 1 and exon 4 of each of the four CYP3A isoforms (Table 2) were used at a final concentration of 250 nM. Reactions were performed in triplicate with the QuantiTect SYBR Green one step RT-PCR kit (Qiagen) on a DNA Engine Opticon 2 instrument (MJ Research, Boston, MA). Serial dilutions of PCR amplicons for each of the four specific CYP3A isoforms were used to generate standard curves ranging from 100 to 10^7 copies. CYP3A mRNA transcript numbers were calculated from linear regression analysis of the respective standard curves. Data were normalized to 18S rRNA using the TaqMan Ribosomal RNA Control Reagent kit (Applied Biosystems, Foster City, CA).

Specificity of the assays for the four CYP3A isoforms was confirmed by sequencing the amplicons and further determined by comparative QRT-PCR experiments wherein each CYP3A isoform-specific primer set was tested for specificity against 10^6 molecules of CYP3A4,

CYP3A5, CYP3A7 and CYP3A43 templates. When the CYP3A7 primer set was used under the experimental conditions described above, a cycle threshold (Ct) difference of >14 cycles was observed between the CYP3A7 template and the other three templates (*i.e.* Ct values were >14 cycles greater for CYP3A4, CYP3A5 and CYP3A43 than that observed with the CYP3A7 template). Using the CYP3A4, CYP3A5 and CYP3A43 primer sets, differences in Ct values were greater than 13 cycles between the cognate and alternative targets.

Preparation of Anti-CYP3A7/4 Antibody. The primary antibody was raised in rabbits against the C-terminal pentapeptide of CYPs 3A4 and 3A7, Thr-Val-Ser-Gly-Ala that had been conjugated to keyhole limpet hemocyanin (KLH) using Sulfo-SMCC chemistry via a cysteine residue added to the *N*-terminus of the pentapeptide. Pathogen-free New Zealand White rabbits (HsdOkd:NZW) were immunized with 1 mg of peptide-KLH antigen emulsified in Freund's Complete Adjuvant followed by secondary immunizations on days 28, 56 and 84. Production bleeds (~25 ml) were obtained on day 98 and day 105 followed by complete exsanguination on day 112. Antigen preparation and antibody production was carried out by Harlan Bioproducts (Indianapolis, IN).

To minimize non-specific binding, the anti-peptide antibody was affinity purified using the PinPoint™ Xa Protein Purification System (Promega, Madison, WI). Oligonucleotides (sense, 5'-AGCTTTGCACCGTGAGCGGCGCGTAAG-3' and antisense, 5'-GATCCTTACGCGCCGC TCACGGTGCAA-3') encoding the CYP3A4/7 pentapeptide were synthesized (Sigma-Genosys, The Woodlands, TX), allowed to anneal, phosphorylated with T4 polynucleotide kinase, and ligated into the PinPoint™ Xa-3 vector between the *Hind*III and *Bam*HI restriction sites to create an in-frame fusion with the biotinylated target sequence encoded by the vector. Clones were sequenced to confirm the presence of the oligonucleotide insert. The pentapeptide epitope was

expressed in *E. coli* as the C-terminus of a biotinylated fusion protein. An affinity column was prepared by immobilization of the biotinylated fusion protein on TetraLink™ Tetrameric Avidin Resin (Promega). Anti-peptide antibodies were allowed to bind to the fusion protein solid phase, the column washed with >5 bed volumes of buffer, and bound antibodies eluted with 100 mM glycine, pH 2.8. The antibody was specific for CYP3A4 and 3A7, and did not react with heterologously expressed CYPs 1A1, 1A2, 2A6, 2B6, 2C8, 2C9, 2C19, 2D6, 2E1, or 3A5.

Immunoquantitation of Microsomal CYP3A7/4 Protein. Fetal liver microsomes were diluted in sample buffer (10% glycerol, 141 mM Tris base, 106 mM Tris HCl, 2% LDS, 0.51 mM EDTA, 0.22 mM SERVA Blue G250, 0.175 mM Phenol Red) containing fresh 50 mM DTT and heated for 10 minutes at 70° C. Microsomal proteins, 0.5 µg per lane, were separated on 4-15% Criterion 26-well gels in running buffer (25 mM Tris, 192 mM glycine and 0.1% w/v SDS, pH 8.3) at 200 V for 45 minutes. Proteins were transferred to nitrocellulose membranes using a Bio-Rad Semi-dry transfer unit with transfer buffer containing 39 mM glycine, 48 mM Tris, 0.0375% SDS and 20% methanol. Membranes were blocked overnight at room temperature on a rocker in 10 mM Tris, 150 mM NaCl, 0.2% Tween-20, pH 8.0 (TNT) containing 4% skim milk powder (M-TNT). Blocked membranes were incubated for 1 h with affinity-purified anti-CYP3A7/4 antibody diluted 1:20,000-fold in M-TNT and washed with TNT (5 min x 6). To detect bound antibody, blots were incubated with HRP-conjugated donkey anti-rabbit antibody (1:50,000) in M-TNT for 30 min, washed (5 min x 6), incubated with ECL Plus chemiluminescence reagents according to the manufacturer's directions (Amersham Biosciences) and exposed on Hyperfilm ECL. Films were scanned using a flat-bed scanner, and densitometric analysis of immunoreactive protein was conducted using Kodak Digital Science 1D Image Analysis Software, version 3.6 (Eastman Kodak Company, Rochester, NY). Standard curves (0.025 pmol

to 0.3 pmol per lane heterologously expressed CYP3A7; BD Gentest) were present on each membrane. Standard curves were linear over the range of standards, and coefficients of determination (r^2 values) ranged from 0.972 to 0.999. Back-extrapolated values for the standards expressed as a percentage of the nominal values ranged from 3.6% to 8.8% between 0.3 pmol and 0.05 pmol, while a value of 29.9% was obtained for the 0.025 pmol standard. Values presented are the mean of duplicate determinations.

Incubation Conditions for Catalytic Activity Assays. *In vitro* enzyme assays were performed in 96-well microtiter plates. Standard incubation reactions (100 µl) contained microsomes prepared from fetal human liver (5-50 µg of microsomal protein) or insect cell microsomes containing baculovirus-expressed cytochrome P450 enzymes (1-5 pmol) co-expressed with P450 reductase, potassium phosphate buffer (50 mM, pH 7.4), $MgCl_2$ (3 mM), EDTA (1 mM), and substrate (250 µM testosterone; 100 µM DHEA). Reactions were initiated by the addition of an NADPH-generating system, consisting of NADP (1 mM), glucose-6-phosphate (1 U/ml), and glucose-6-phosphate dehydrogenase (5 mM), placed in a Thermo Forma (Marietta, OH) Benchtop Orbital Shaker incubator at 37±0.1°C, and terminated after 10-30 min by the addition of 100 µl of ice-cold methanol. Protein was precipitated by centrifugation at 10,000 g_{max} for 10 min. An aliquot (20-100 µl) of the supernatant was analyzed by reversed-phase HPLC via direct injection. Under these conditions, metabolism of the parent compounds did not exceed 20 per cent and rates of metabolite formation were proportional to incubation time and protein concentration. Duplicate determinations were performed for each sample.

Analytical Methods. HPLC analyses were performed with a Hewlett Packard HP1100 HPLC system with programmable 1100 series diode array and fluorescence detectors (Hewlett Packard

Instruments, Santa Clara, CA). All data were collected and integrated with Hewlett Packard Chemstation V A.0401 software. Testosterone and its 2α-, 2β-and 6β-hydroxylated metabolites were resolved by reverse phase HPLC via direct injection according to the method of Purdon and Lehman-McKeeman (Purdon and Lehman-McKeeman, 1997), as modified by Usmani *et al* (Usmani et al., 2003). Under these conditions, 6α-, 15α-, 6β-, 2α-, and 2β-hydroxytestosterone, androstenedione and testosterone had retention times of 14.8 min, 15.9 min, 16.4 min, 20.8 min, 21.6 min, 25.0 min and 28.0 min, respectively. The solvent program was modified slightly such that 16αDHEA eluted at 17.0 min and DHEA eluted at 27.2 min. The analytical methods demonstrated linearity (r^2 = 0.999) over the range of standards evaluated (5 pmol to 1250 pmol of testosterone metabolites and 5 pmol to 1500 pmol of 16αDHEA injected).

Genomic DNA Isolation and Genotyping for *CYP3A7*1B, *1C, *1E* Allelic Variants. Genomic DNA was isolated from 5-25 mg tissue using a DNeasy Tissue Kit (Qiagen). *CYP3A7*1C* genotyping was adapted from Burk *et al* (Burk et al., 2002) with the following modifications: a 2468 bp long fragment was amplified from genomic DNA in a 15 µl reaction using JumpStart REDTaq DNA polymerase (Sigma, St Louis, MO), the buffer provided with the enzyme and 0.2 µM of each primer (listed in Table 2). After PCR amplification, 12 µl of a mixture containing 2.5 units of *Ssp*I and NEB digestion buffer "U" (New England Biolabs, Beverly, MA) was added to each reaction and incubated overnight at 37ºC. Restriction fragments were separated on an agarose gel by electrophoresis and documented with a Kodak 440 CF Image Station (Eastman Kodak Co., New Haven, CT). A *CYP3A7*1/*1C* sample was included as a positive control.

JPET Fast Forward. Published on April 21, 2005 as DOI: 10.1124/jpet.105.086504
This article has not been copyedited and formatted. The final version may differ from this version.

To confirm the *CYP3A7*1C* genotype and to genotype for *CYP3A7*1B, *1D,* and **1E* alleles, genomic DNA was amplified with JumpStart RED*Taq* DNA Polymerase (Sigma) and 0.2 µM oligonucleotide primers 3A7 197291-F (5'-CACCTCTGCTAAGGGAAACAGGCC) and 3A7 198150-R (5'-GCCAGCCTGAACATCCTTTTTGCTA). Specificity of both PCR primers was achieved by aligning the four *CYP3A* genes and the two pseudogene sequences *CYP3AP1* and *CYP3P2* using the LAGAN algorithm (Brudno et al., 2003). The 859 bp amplicon encompassing 680 bp of the proximal promoter, exon 1 and 109 bp of intron 1 was treated with ExoSAP-IT (USB, Cleveland, OH) and subsequently sequenced with the DYEnamic ET Dye Terminator Cycle Sequencing Kit for MegaBACE (Amersham Biosciences). Unincorporated fluorescent dye-terminators were removed from the reactions by solid-phase magnetic CleanSEQ beads (Agencourt, Beverly, MA) according to the manufacturer's recommendations prior to analysis on a MegaBACE 500 DNA Analysis System. The data were analyzed with the Phred/Phrap/Consed software package (University of Washington, Seattle, WA).

Genotyping for *CYP3A7*2* by XL-PCR sequencing. To detect the g.26041C>G (Thr409Arg) variant, a *CYP3A7* specific 6.51 kb long PCR amplicon including exons 11-13 was generated with Platinum *Taq* DNA Polymerase High Fidelity (Invitrogen, Carlsbad, CA) and primers 3A7 223378-F (5' CAATAATCCTTGTCGCACAGAGAATTTG) and 3A7 229891-R (5' ATAATTTGGAGTTATCATTTGGAGGGTCT). Reaction conditions were as follows: denaturing, 94ºC for 20s, annealing, 64ºC for 30s and extension, 68ºC for 6 min, for 40 cycles. The GenBank entry NG_000004.2 was used to design the amplification primers. The PCR reaction was subsequently cleaned up as described above and a 0.8 µl aliquot was sequenced with primers 3A7 223735-F (5' TCAACAGTACTACATGGACTG) and 3A7 224241-R (5' GGGACTGTGACTGGCTATAG).

Genotyping *CYP3A5* Allelic Variants. PCR-RFLP-based assays for *CYP3A5*3, CYP3A5*4,* and *CYP3A5*5* were adapted from published methods (van Schaik et al., 2002) or developed *de novo* (*CYP3A5*2, CYP3A5*6* and *CYP3A5*7*). Complete assay details are presented in Table 3. Assays for *CYP3A5*2, CYP3A5*3* and *CYP3A5**7 were conducted using genomic DNA with 40 cycles of amplification. Improved assay performance for the *CYP3A5*4, CYP3A5*5* and *CYP3A5*6* alleles was achieved using a 8152 bp long *CYP3A5*-specific template generated with Platinum *Taq* DNA polymerase High Fidelity according to the manufacturer's recommendations (Invitrogen) with 10 sec annealing at 70ºC and 9 min extension at 68ºC for 35 cycles (primers listed in Table 3). All other PCR reactions were conducted with JumpStart REDTaq DNA polymerase (Sigma) using the buffer provided with the enzyme except for the *CYP3A5*7* product, which was generated using FailSafe buffer C (Epicentre, Madison, WI). After PCR amplification, an equal volume (8 µl) containing the relevant restriction enzyme (NEB and Amersham) and digestion buffer was added to each reaction and incubated for at least 2 h. PCR-RFLP fragments were separated by gel electrophoresis (3% agarose gels containing Synergel, Diversified Biotech, Boston, MA) and documented as described above.

Statistical Analysis. Results are reported as the mean ± SD. Measures of linkage disequilibrium were determined using Haploview version 3.11 (Barrett et al., 2004). Univariate linear regression and ANOVA with Tukey's post-hoc analysis were conducted using SPSS version 12 for Windows (SPSS Inc., Chicago, IL). $p<0.05$ was accepted as a statistically significant difference.

Results

Variability in CYP3A Gene Transcription in Human Fetal Liver: Expression of CYP3A mRNAs is reported as transcripts/ng total RNA corrected for the expression of 18S rRNA as recommended by Koch *et al.* (Koch et al., 2002). Although RNA quality demonstrated some variability across the panel of specimens, prominent 18S and 28S bands were evident in all samples (not shown), and values for 18S rRNA expression varied only 3.9-fold in this sample set (mean ± SD, 4.97 ± 1.55 x 10^7 transcripts/ng total RNA; range, 2.48 x 10^7 to 9.73 x 10^7 transcripts/ng total RNA).

CYP3A7 transcripts were the most abundant of the individual CYP3A isoforms (Fig. 1) and expression varied 634-fold in this panel of human fetal liver samples. Mean ± SD (range) expression was 14,200 ± 15,000 transcripts/ng total RNA (151 to 95,700 transcripts/ng total RNA; Table 4). A subset of samples had markedly reduced levels of CYP3A7 mRNA, protein and activity (*vide infra*). When these five samples were excluded from the analysis, variability in CYP3A7 mRNA expression decreased from 634- to 72-fold. On an individual basis, CYP3A5 mRNA expression was, on average, 100-fold lower than CYP3A7 expression and varied 123-fold (254 ± 321 transcripts/ng total RNA; range 13.5 to 1,670 transcripts/ng total RNA) across the full panel. CYP3A4 mRNA expression was approximately 1,000-fold lower than CYP3A7 expression and varied 10.3-fold (15.1 ± 8.9 transcripts/ng total RNA; range 4.7 to 48.2 transcripts/ng total RNA). Expression of CYP3A43 mRNA was similar to that observed for CYP3A4. There was no relationship between the expression of CYP3A7 and either CYP3A5 (r^2=0.103) or CYP3A4 (r^2=0.080) nor was the expression of any CYP3A mRNA associated with estimated gestational age (EGA; Fig. 1).

Variability in CYP3A7/4 Immunoreactive Protein. Immunoreactive CYP3A7/4 protein content was determined for 51 of the 54 fetal liver samples and averaged 234.8 ± 123.1 pmol CYP3A7/4 protein/mg microsomal protein (Table 4). A representative immunoblot (standard curve: r^2=0.972) illustrating a range of immunoreactive protein contents is presented in Fig 2A. CYP3A7 remained undetectable in one sample (CMM1153) even when the amount of protein loaded was increased 4-fold to 2 µg/lane. For samples with detectable protein, CYP3A7/4 content varied 21.6-fold from 20.6 to 439.9 pmol/mg microsomal protein. Although samples with the lowest CYP3A7 mRNA expression also had the lowest immunoreactive CYP3A7/4 protein expression, the overall correlation was poor (r^2=0.129). Likewise, immunoreactive CYP3A7/4 protein across all samples was poorly correlated with EGA (r^2=0.149; Fig 2B). Significant correlations were, however, observed between protein content and both testosterone 2α-hydroxylation (T2αH; r^2=0.541, p<0.01; Fig. 2C) and DHEA 16α-hydroxylation (DHEA16αH; r^2=0.585, p<0.01; Fig. 2D) activities.

Testosterone Biotransformation. Since published data indicated that human CYP3A isoforms demonstrated regiospecific patterns of testosterone biotransformation (Usmani et al., 2003), we investigated the potential for testosterone 6β-hydroxylation (T6βH) and T2αH activities to determine the relative contributions of CYP3A isoforms towards catalytic activities in human fetal liver. Product formation using heterologously expressed rCYP3A4, rCYP3A5 and rCYP3A7 (and experimental conditions identical for those to be employed for incubations containing fetal liver microsomal protein) are presented in Table 5. The ratio of T2αH and T6βH activities (T2αH/T6βH ratio) appeared to be particularly useful for discriminating among the three CYP3A isoforms since the rCYP3A7 value of 1.19 was an order of magnitude greater

than the rCYP3A5 value of 0.079, which was approximately 10-fold greater than the ratio of 0.007 determined with rCYP3A4 (Table 5).

In the fetal liver microsomal samples, the T2αH/T6βH ratio was 1.71 ± 0.32 with a minimum value of 0.54 and a maximum value of 2.14 (Fig. 3). The value of 1.19 associated with rCYP3A7 was exceeded in 49/51 samples, the exceptions being samples with values of 0.54 and 1.17, respectively. The lowest ratio, 0.54, was observed in a sample with very low T2αH and T6βH activities of 6.4 and 11.9 pmol/min/mg protein, respectively. To address potential contributions from CYP3A5, the samples were genotyped for the *CYP3A5* intron 3 polymorphism (g.6986A>G). ANOVA revealed a statistically significant inverse relationship between the T2αH/T6βH ratio and the number of functional g.6986A alleles (reference sequence as defined by the Human Cytochrome P450 Nomenclature Committee; http://www.imm.ki.se/CYPalleles/cyp3a5.htm; F=7.01, p=0.002; not shown). The presence of functional CYP3A5 protein has been confirmed in these samples by immunoblot analysis and midazolam hydroxylation (data not shown; manuscript in preparation). Although considerable overlap among groups was observed, post-hoc analysis with Tukey's HSD confirmed that at least one g.6986A allele resulted in significantly lower ratio values compared to two g.6986G alleles. It should be noted that both *CYP3A5*1* and **6* alleles genotype as g.6986A, although the *CYP3A5*6* allele is associated with reduced activity due to an additional downstream splicing defect (Rogan et al., 2003). For the sample with the lowest T2αH/T6βH ratio, the contribution of CYP3A5 likely is minimal since this sample was genotyped as *CYP3A5*3/*6* and neither immunoreactive CYP3A5 protein, nor midazolam hydroxylation activity was detected (not shown).

T2αH activity varied approximately 175-fold from 3.6 pmol/min/mg to 642.9 pmol/min/mg (323.1 ± 171.1 pmol product formed/min/mg microsomal protein); the majority (46/51) of samples fell within a 6.7-fold range with five samples displaying markedly reduced activities. Similarly, T6βH activity varied 167-fold (186.6 ± 105.5 pmol/min/mg; range 2.6 to 439.4 pmol/min/mg) and decreased to 9.1-fold in the absence of the low activity subgroup. A strong correlation was observed between T6βH and T2αH activities (r^2=0.859; Fig. 4A), with the greatest deviations from the fitted model parameters occurring in those samples with the highest T2αH activities. For those livers in which CYP3A5 protein theoretically should be expressed (at least one g.6986A allele; solid symbols, Fig. 4A), the coefficient of determination was essentially identical to that observed with the entire data set (r^2=0.861). Moreover, in the subset of samples genotyped as *CYP3A5*3/*3* (n=28), T2αH and T6βH activities were almost exclusively catalyzed by a single enzyme (r^2=0.974; open symbols, Fig. 4A). In Fig. 4A, those samples genotyped as *CYP3A5*3/*6* tended to associate more with the *CYP3A5*3/*3* samples while the sole *CYP3A5*6/*6* specimen fell close to the line of best fit for the g.6986A group. A weak (r^2=0.194) but statistically significant (F=11.83, p=0.0012) relationship was observed between T2αH activity and EGA. However, removal of the set of samples with extremely low activity abolished the statistical significance.

DHEA 16α-Hydroxylase (DHEA16αH) Activity. Fetal liver microsomes were more active towards DHEA as a substrate than towards testosterone. Mean ± SD DHEA16αH activity was 7.30 ± 3.61 nmol product formed/min/mg microsomal protein. Values varied approximately 250-fold ranging from 0.059 to 14.91 nmol/min/mg when all samples were included in the analysis but varied only 6.2-fold when the low activity samples were excluded. DHEA16αH

activity was significantly correlated with T2αH activity (r^2=0.856, p<0.0001) but was not affected by *CYP3A5* genotype (Fig. 4B). A weak (r^2=0.256) but statistically significant (F=15.96, p=0.0002) correlation was observed between DHEA16αH activity and EGA but as observed for T2αH activity, this relationship was dependent upon the presence of the set of samples with extremely low activity (not shown). There was no relationship between DHEA16αH activity and the total length of time that the tissues were stored prior to isolation of microsomes (r^2=0.002).

Association of *CYP3A7* Allelic Variants with Measures of *CYP3A7* Expression. Since DHEA16αH activity did not appear to be influenced by *CYP3A5* genotype, subsequent phenotype-genotype correlations were evaluated using this measure. No *CYP3A7*1B, *1C* or **1D* alleles were observed in this sample set, while three African American and one Caucasian sample, were heterozygous for the *CYP3A7*1E* allele (*f*=0.037). No relationship between *CYP3A7*1E* and DHEA16αH activity was apparent (values of 0.09, 4.4, 9.0 and 12.4 nmol/min/mg.

The frequency of the *CYP3A7*2* allele in this set of fetal samples was 0.378, and was in linkage disequilibrium with *CYP3A5*3* (D'=0.90 with 95% confidence interval 0.76 to 0.93; r^2=0.74). No association was observed between DHEA16αH activity and the number of *CYP3A7*2* alleles by ANOVA (F=0.326, *p*=0.724; Fig. 5).

Discussion

Historically, CYP3A7 has been considered a "fetal-specific" form of cytochrome P450 but little is known concerning the extent of "normal" variation in its expression or the genetic and environmental determinants underlying that variability. Stevens *et al.* have identified several critical technical and logistical issues contributing to this knowledge deficit including 1) limited numbers of samples within targeted developmental stages; 2) difficulty acquiring tissues of sufficiently high quality to generate meaningful data in *in vitro* studies; and 3) an inability to accurately and reliably ascertain the relative contributions of CYPs 3A4 and 3A5 to observed CYP3A7 activity using currently available substrates and reagents (Stevens et al., 2003).

Although 170- to 250-fold variability in testosterone and DHEA hydroxylation and 634-fold variability in CYP3A7 mRNA expression was observed across the entire panel, most of this variability could be attributed to the presence of a subset (n=5) of samples with extremely low values. Variability in catalytic activity was 10-fold or less for the remaining samples (Table 4). It is unlikely that poor sample quality was a major factor contributing to the observed interindividual variability for several reasons. The post mortem interval was 2 h or less for 49 of the 54 samples. Furthermore, 18S rRNA values demonstrated minimal (3.9-fold) variation, consistent with the observations of Koch *et al.* in adult liver (Koch et al., 2002), and no correlation was observed between either the post mortem interval or 18S rRNA value and any measure of CYP3A7 expression.

A major concern in characterizing the extent of variability in CYP3A7 activity has been ascertaining the contribution of even minimal amounts of CYP3A4 (or CYP3A5) present in a sample due to the overlapping activities towards probe substrates by these closely related

CYP3A isoforms, and the lack of specificity of antibody reagents used for immunoquantitation (Stevens et al., 2003). In the set of fetal liver samples investigated for this report, expression of CYP3A4 appeared to be minimal based on relative mRNA expression and catalytic activity towards testosterone. The average T6βH activity in this panel of fetal liver microsomes was 186.6 pmol/min/mg protein with a maximum value of 439.4 pmol/min/mg, markedly lower than activities of approximately 800 to 14,000 pmol/min/mg reported in adult liver microsomes (Pearce et al., 1996). Observed regiospecific patterns of testosterone hydroxylation also were more consistent with a pattern of catalysis dominated by CYP3A7 activity rather than by CYP3A4 activity (Usmani et al., 2003). For example, T2αH activity measured in fetal liver microsomes exceeded T6βH activity in all samples but one, and in 49/51 samples the observed T2αH/T6βH ratio was greater than the value of 1.186 established with rCYP3A7. Moreover, the lowest observed ratio in fetal liver microsomes, 0.535, was considerably greater than the values of 0.079 and 0.007 observed with rCYP3A5 and rCYP3A4, respectively. Finally, visual inspection of HPLC chromatograms from analyses of DHEA biotransformation failed to reveal any peaks that would correspond to 7β-hydroxyDHEA formation by fetal liver microsomes, a product that is highly specific to CYP3A4 (Stevens et al., 2003).

In contrast, CYP3A5 may be more likely to confound estimates of CYP3A7 expression since CYP3A5 immunoreactive protein has been detected in approximately 50% of fetal liver microsomal samples (Hakkola et al., 2001; Stevens et al., 2003). In our panel, genotyping for *CYP3A5* g.6986A>G identified a subset of samples where the expression of CYP3A5 protein was predicted to be negligible (*CYP3A5*3/*3*). The high correlation between T2αH and T6βH activities (r^2=0.974) for *CYP3A5*3* homozygotes strongly suggests that a single enzyme, CYP3A7, was primarily responsible for both activities. In contrast, DHEA16αH activity was

not affected by *CYP3A5* genotype providing support that it is a more specific marker of CYP3A7 activity than testosterone in fetal liver microsomes *i.e.* under conditions where CYP3A4 expression is minimal or absent. The fact that *CYP3A5* genotyping segregates testosterone hydroxylation activity, but not DHEA16αH activity, into two groups suggests that CYP3A5 may contribute to the biotransformation of some substrates but not others in fetal liver. A more detailed characterization of CYP3A5 activity in this panel is currently in preparation.

Our estimate of average CYP3A7 content in fetal liver microsomes is in agreement with one published report (Stevens et al., 2003) but higher than that reported by others (Lacroix et al., 1997). Stevens *et al.* exploited differential patterns of DHEA 16α- and 7β-hydroxylation by CYP3A7 and CYP3A4 in conjunction with a validated nonlinear multivariate regression model to calculate CYP3A4 and CYP3A7 protein in a subset of pre- and postnatal livers. Using this innovative, but indirect, measure, they observed an average CYP3A7 content of 311 pmol/mg microsomal protein in the second trimester, 201 pmol/mg in the third trimester, and 158 pmol/mg in premature birth samples, suggesting that increasing gestational age may also contribute to the observed variability in CYP3A7 expression (Stevens et al., 2003). Published data are conflicting in this regard (Lacroix et al., 1997), and only a weak association between EGA and CYP3A7 activity was observed across the entire panel of samples in our investigation due, most likely, to the limited number of late term samples. Nevertheless, it is likely that factors other than EGA are responsible for the extremely low values of CYP3A7 activity observed in our study since Stevens *et al.* reported only a 50% decrease in CYP3A7 content between second trimester samples and samples from prematurely born infants (Stevens et al., 2003).

Since CYP3A5 genotype did not have any discernable effect on DHEA16αH activity, this measure was considered to best reflect variability in CYP3A7 expression. We speculate that the extreme range observed in the current study does not reflect "normal" variability in fetal liver CYP3A7 activity since variability was only 6.2-fold when the subset of low samples was excluded. Furthermore, three of the samples in the "low activity" group were obtained from fetuses with severe congenital anomalies – anencephaly, porencephaly and hydrops fetalis. Although hepatic dysfunction generally is not considered to be associated with either anencephaly or porencephaly, hypothalamic-pituitary function is disrupted in anencephalic fetuses such that ACTH levels are insufficient to support fetal adrenal development as inferred from dramatically reduced maternal estrogen concentrations (Mesiano and Jaffe, 1997). While regulation of estrogen biosynthesis is severely dysregulated under these conditions, the effects on CYP3A7 activity are less clear. Milewich *et al* observed that 16α-hydroxylase activity towards estrone sulfate and estradiol sulfate was similar in anencephalic fetuses (gestational ages not reported) compared to "normal" fetuses, although activities were markedly lower in one of a pair of twin anencephalic fetuses (Milewich et al., 1986). However, the relative paucity of available information makes it impossible to know whether the extremely low CYP3A7 activity was due to fetal pathology or poor tissue quality (subject to the considerations discussed above). The 6- to 7-fold variation in activity observed in the majority of samples more likely represents true variability within the viable fetal population.

Persistence of CYP3A7 mRNA expression postnatally has been associated with the presence of the *CYP3A7*1C* allele (Kuehl et al., 2001). No *CYP3A7*1C* alleles were observed among our 54 fetal samples although we have observed an allele frequency of 2.3% in an African American control population (n=87). Thus, the *CYP3A7*1C* allele does not contribute to the observed

variability in mRNA expression or catalytic activity observed in fetal liver. Genotyping for the previously described *CYP3A7*2* allele (Rodriguez-Antona et al., 2005) also could not account for the variation observed in any of the *in vitro* phenotypic measures investigated. Although Rodriguez-Antona *et al.* reported moderately higher DHEA hydroxylation for the *CYP3A7*2* allele (Rodriguez-Antona et al., 2005), the tendency of this allele to demonstrate higher DHEA16αH activity among our fetal panel did not achieve statistical significance. However, genotype-phenotype correlations may be obscured by the fact that CYP3A7 activity has been reported to be activated by steroid sulfate conjugates, such as pregnenolone 3-sulfate, 17α-hydroxypregnenolone 3-sulfate and DHEA-S, but not the corresponding unconjugated forms (Nakamura et al., 2003). Thus, activity/phenotype of the wild-type and variant proteins may be differentially affected by the specific substrate concentration used in the *in vitro* analyses.

The overall variability in CYP3A7 activity observed in this study may seem inconsistent with an important physiological function but exclusion of a low activity subgroup resulted in only 6- to 7-fold variability in catalytic activity. Comparative analyses revealed that *in vitro* clearance of prototypic CYP3A substrates is generally 5- to 10-fold lower for CYP3A7 compared to CYP3A4 (Williams et al., 2002), implying a primarily physiological role for CYP3A7 in fetal liver. Given the importance of CYP3A7 to estriol biosynthesis during pregnancy and its potential to provide protection against exogenous sources of retinoic acid esters, a thorough understanding of allelic variation, alternative splicing and developmental expression of *trans*-acting factors potentially involved in regulating CYP3A7 expression, such as PXR, CAR, RXR, and the vitamin D receptor (VDR), is warranted and relevant investigations currently are in progress.

References

Barrett JC, Fry B, Maller J and Daly MJ (2005) Haploview: analysis and visualization of LD and haplotype maps. *Bioinformatics* **21**:263-265.

Baulieu EE and Dray FL (1963) Conversion of ^{3}H-dehydroepiandrosterone (3β-hydroxy-5-androsten-17-one) sulfate to ^{3}H-estrogens in normal pregnant women. *J Clin Endocrinol Metab* **23**:1298-1301.

Brudno M, Do C, Cooper G, Kim MF, Davydov E, Green ED, Sidow A and Batzoglou S (2003) LAGAN and Multi-LAGAN: efficient tools for large-scale multiple alignment of genomic DNA. *Genome Res* **13**:721-731.

Burk O, Tegude H, Koch I, Hustert E, Wolbold R, Glaeser H, Klein K, Fromm MF, Nuessler AK, Neuhaus P, Zanger UM, Eichelbaum M and Wojnowski L (2002) Molecular mechanisms of polymorphic *CYP3A7* expression in adult human liver and intestine. *J Biol Chem* **277**:24280-24288.

Chen H, Fantel AG and Juchau MR (2000) Catalysis of the 4-hydroxylation of retinoic acids by CYP3A7 in human fetal hepatic tissues. *Drug Metab Disp* **28**:1051-1057.

Hakkola J, Raunio H, Purkunen R, Saarikoski S, Vähäkangas K, Pelkonen O, Edwards RJ, Boobis AR and Pasanen M (2001) Cytochrome P450 3A expression in the human fetal liver: Evidence that CYP3A5 is expressed in only a limited number of fetal livers. *Biol Neonate* **80**:193-201.

Kitada M, Kamataki T, Itahashi K, Rikihisa T and Kanakubo Y (1987) P-450 HFLa, a form of cytochrome P-450 purified from human fetal livers, is the 16α-hydroxylase of dehydroepiandrosterone 3-sulfate. *J Biol Chem* **262**:13534-13537.

Koch I, Weil R, Wolbold R, Brockmöller J, Hustert E, Burk O, Nuessler AC, Neuhaus P, Eichelbaum M, Zanger UM and Wojnowski L (2002) Interindividual variability and tissue-specificity in the expression of cytochrome P450 3A mRNA. *Drug Metab Disp* **30**:1108-1114.

Kuehl P, Zhang J, Lin Y, Lamba J, Assem M, Schuetz J, Watkins PB, Daly AK, Wrighton SA, Hall SD, Maurel P, Relling M, Brimer C, Yasuda K, Venkataramanan R, Strom S, Thummel KE, Boguski MS and Schuetz E (2001) Sequence diversity in *CYP3A* promoters and characterization of the genetic basis of polymorphic CYP3A5 expression. *Nat Genet* **27**:383-391.

Lacroix D, Sonnier M, Moncion A, Cheron G and Cresteil T (1997) Expression of CYP3A in the human liver. Evidence that the shift between CYP3A7 and CYP3A4 occurs immediately after birth. *Eur J Biochem* **247**:625-634.

Li Y, Yokoi T, Katsuki M, Wang JS, Groopman JD and Kamataki T (1997) In vivo activation of aflatoxin B1 in C57BL/6N mice carrying a human fetus-specific CYP3A7 gene. *Cancer Res* **57**:641-645.

Lu AYH and Levin W (1972) Partial purification of cytochromes P-450 and P-448 from rat liver microsomes. *Biochem Biophys Res Commun* **46**:1334-1339.

Marill J, Capron CC, Idres N and Chabot GG (2002) Human cytochrome P450s involved in the metabolism of 9-cis- and 13-cis-retinoic acids. *Biochem Pharmacol*.**63**:933-943.

Marill J, Cresteil T, Lanotte M and Chabot GG (2000) Identification of human cytochrome P450s involved in the formation of all-*trans*-retinoic acid principal metabolites. *Mol Pharmacol* **58**:1341-1348.

Mesiano S and Jaffe RB (1997) Developmental and functional biology of the primate fetal adrenal cortex. *Endocrine Rev.***18**:378-403.

Milewich L, MacDonald PC, Guerami A, Midgett WT, Lassiter WI and Carr BR (1986) Human fetal liver estrogen 16α-hydroxylase: Precursor specificity, kinetic parameters, and *in vitro* regulation. *J Clin Endocrinol Metab* **63**:180-191.

Nakamura H, Torimoto N, Ishii I, Ariyoshi N, H. N, Ohmori S and Kitada M (2003) CYP3A4 and CYP3A7-mediated carbamazepine 10,11-epoxidation are activated by differential endogenous steroids. *Drug Metab Disp* **31**:432-438.

Nebert DW (1991) Proposed role of drug-metabolizing enzymes: Regulation of steady state levels of the ligands that effect growth, homeostasis, differentiation, and neuroendocrine functions. *Mol Endocrinol* **5**:1203-1214.

Nebert DW (1994) Drug-metabolizing enzymes in ligand-modulated transcription. *Biochem Pharmacol* **47**:25-37.

Pearce RE, McIntyre CJ, Madan A, Sanzgiri U, Draper AJ, Bullock PL, Cook DC, Burton LA, Latham J, Nevins C and Parkinson A (1996) Effects of freezing, thawing, and storing human liver microsomes on cytochrome P450 activity. *Arch Biochem Biophys* **331**:145-169.

Purdon MP and Lehman-McKeeman LD (1997) Improved high-performance liquid chromatographic procedure for the separation and quantification of hydroxytestosterone metabolites. *J Pharmacol Toxicol Methods* **37**:67-73.

Rodriguez-Antona C, Jande M, Rane A and Ingelman-Sundberg M (2005) Identification and phenotype characterization of two *CYP3A* haplotpyes causing different enzymatic capacity in fetal livers. *Clin Pharmacol Ther* **77**:259-270.

Rogan PK, Svojanovsky S and Leeder JS (2003) Information theory-based analysis of *CYP2C19, CYP2D6* and *CYP3A5* splicing mutations. *Pharmacogenetics* **13**:207-218.

Ryan KJ (1959) Metabolism of C-16 oxygenated steroids by human placenta. The formation of estriol. *J Biol Chem* **234**:2006-2008.

Schuetz JD, Kauma S and Guzelian PS (1993) Identification of the fetal liver cytochrome CYP3A7 in human endometrium and placenta. *J Clin Invest* 92:1018-1024.

Serón-Ferré M and Jaffe RB (1981) The fetal adrenal gland. *Annu. Rev. Physiol*. **43**:141-162.

Siiteri PK and MacDonald PC (1963) The utilization of circulating dehydroepiandrosterone sulfate for estrogen synthesis during human pregnancy. *Steroids* **2**:713-730.

Stevens JC, Hines RN, Gu C, Koukouritaki SB, Manro JR, Tandler PJ and Zaya MJ (2003) Developmental expression of the major human hepatic CYP3A enzymes. *J Pharmacol Exp Ther* **307**:573-582.

Usmani KA, Rose RL and Hodgson E (2003) Inhibition and activation of the human liver microsomal and human cytochrome P450 3A4 metabolism of testosterone by deployment-related chemicals. *Drug Metab Disp* **31**:384-391.

van Schaik RHN, van der Heiden IP, van den Anker JN and Lindemans J (2002) *CYP3A5* variant allele frequencies in Dutch Caucasians. *Clin Chem* **48**:1668-1671.

Williams JA, Ring BJ, Cantrell VE, Jones DR, Eckstein J, Ruterbories K, Hamman MA, Hall SD and Wrighton SA (2002) Comparative metabolic capabilities of CYP3A4, CYP3A5 and CYP3A7. *Drug Metab Disp* **30**:883-891.

Yang H-YL, Lee QP, Rettie AR and Juchau MR (1994) Functional cytochrome P4503A isoforms in human embryonic tissues: Expression during organogenesis. *Mol Pharmacol* **46**:922-928.

Footnotes

Supported by grant R01 ES10855-04 from the National Institute of Environmental Health Sciences

Reprint requests: J Steven Leeder, Section of Developmental Pharmacology and Experimental Therapeutics, Children's Mercy Hospital and Clinics, 2401 Gillham Road, Kansas City, MO 64108

Legends to Figures

Figure 1. Comparative expression of CYP3A7 (solid inverted triangles), CYP3A5 (open circles), CYP3A4 (solid circles) and CYP3A43 mRNA (open inverted triangles) in human fetal liver relative to estimated gestational age (EGA). Data are expressed as transcripts per ng/total RNA and are normalized for 18S ribosomal RNA content.

Figure 2. CYP3A7/4 immunoreactive protein in fetal liver. Immunoreactive CYP3A7/4 protein content was determined using an affinity purified anti-C-terminal peptide antibody that did not differentiate between CYP3A7 and CYP3A4. A. Representative immunoblot containing a 5-point standard curve from 0.025 pmol to 0.3 pmol heterologously expressed CYP3A7 (BD Gentest) per lane. B. Immunoreactive protein content as a function of estimated gestational age (r^2=0.149). C. Correlation between testosterone 2α-hydroxylation activity and immunoreactive protein content (r^2=0.541; p<0.01). D. Correlation between DHEA 16α-hydroxylation activity and immunoreactive protein content (r^2=0.585; p<0.01).

Figure 3. Distribution of the ratio between testosterone 2α-hydroxylase and testosterone 6β-hydroxylase activities in the panel of human fetal liver microsomes. A. Frequency distribution of observed T2αH/T6βH ratios with a Q-Q plot of the same data overlaid. B. Comparison of T2αH/T6βH ratios as a function of the number of *CYP3A5* g.6986A alleles. Individual samples containing no g.6986A alleles are assigned a *CYP3A5*3/*3* genotype (open circles). Samples heterozygous for g.6986A are presented as gray circles while black circles represent homozygous g.6986A samples. Both *CYP3A5*1* and **6* alleles genotype as g.6986A but the *CYP3A5*6* allele is

associated with reduced activity due to a leaky downstream splicing defect (Kuehl et al., 2001; Rogan et al., 2003). Therefore individual samples possessing a *CYP3A5*6* allele are identified by a diagonal white line. One sample has a *CYP3A5*6/*6* genotype (perpendicular diagonal lines). * The T2αH/T6βH ratio for the group with no g.6986A alleles is significantly greater than the other two groups by ANOVA, p=0.002.

Figure 4. A. Correlation between T2αH activity and T6βH activity, and B. between T2αH activity and DHEA16αH activity. Samples were genotyped for the *CYP3A5* g.6986A allele. Samples having at least one *CYP3A5* g.6986A allele are indicated with solid circles while those with two *CYP3A5* g.6986G alleles (assigned a *CYP3A5*3/*3* genotype) are presented as open circles. Samples where the sole "functional" allele is *CYP3A5*6* (*CYP3A5*3/*6* genotypes) are presented as solid circles with a white diagonal line. The sample genotyped as *CYP3A5*6/*6* is indicated by the solid circle with perpendicular diagonal lines.

Figure 5. Relationship between DHEA16αH activity and *CYP3A7* genotype. Presence of the *CYP3A7*2* allele was determined by direct sequencing as described in *Methods*. The subset of samples with extremely low immunoreactive protein and catalytic activity was excluded from the analysis to minimize potential confounding effects such as disease pathology and tissue quality.

Table 1. Demographic data for fetal liver samples.

University of Maryland:					**University of Washington:**				
ID #	**EGA (wk)**	**Gender**	**Race[a]**	**PMI[b] (hr)**	**ID #**	**EGA (wk)**	**Gender**	**Race[a]**	**PMI[b] (hr)**
CMM0032	25	M	CA	2	CMW7470	10.9	M	AA	<2
CMM0045	20	M	AA	2	CMW7480	13.4	M	Unk	<2
CMM0182	16	F	AA	1	CMW7481	11.7	Unk	Unk	<2
CMM0247	19	M	CA	2	CMW7486	15.7	M	CA	<2
CMM0248	20	M	AA	1	CMW7487	12.4	F	Unk	<2
CMM0311	24	F	CA	1	CMW7488	13.0	Unk	Unk	<2
CMM0361	28	M	CA	1	CMW7512	15.4	F	CA	<2
CMM0377	21	F	CA	1	CMW7540	12.7	M	Unk	<2
CMM0379	17	M	AA	1	CMW7541	12.4	Unk	Oth	<2
CMM0532	17	F	AA	1	CMW7554	13.7	Unk	CA	<2
CMM0655	18	F	AA	1	CMW7555	14.0	F	Unk	<2
CMM0684	22	M	CA	5	CMW7556	16.1	F	Unk	<2
CMM0828	19	M	AA	1	CMW7557	13.7	M	Unk	<2
CMM0893	19	F	AA	2	CMW7559	15.4	M	Unk	<2
CMM0908	23	F	CA	3	CMW7566	19.0	F	AA	<2
CMM0978	22	M	CA	6	CMW7567	15.4	F	Oth	<2
CMM1009	27	F	AA	4	CMW7568	12.7	Unk	H	<2
CMM1035	20	F	AA	3	CMW7569	13.4	F	CA	<2
CMM1056	19	F	CA	1	CMW7572	12.1	Unk	NA	<2
CMM1059	20	F	Oth	2	CMW7573	11.4	M	CA	<2
CMM1072	18	M	CA	1	CMW7574	11.1	M	Unk	<2
CMM1087	17	F	AA	2	CMW7575	12.4	Unk	Oth	<2
CMM1106	16	F	AA	1	CMW7576	15.4	M	Oth	<2
CMM1153	32	M	CA	2	CMW7582	13.7	M	AS	<2
CMM1360	16	M	CA	2	CMW7583	15.4	Unk	CA	<2
CMM1388	16	M	AA	1	CMW7584	13.7	Unk	CA	<2
CMM1390	18	F	AA	1					
CMM1411	18	M	AA	1					

[a] AA, African-American; AS, Asian-American; CA, Caucasian-American; H, Hispanic; NA, Native-American; Oth, Other; Unk, gender or ethnic background unknown

[b] PMI: post mortem interval

Table 2. Primers for quantitative PCR of CYP3A mRNA [a]

Gene	Forward Primer (5' to 3')	Reverse Primer (5' to 3')
CYP3A4	CTCTCATCCCAGACTTGGCCA	ACAGGCTGTTGACCATCATAAAAG
CYP3A5	GACCTCATCCCAAATTTGGCGG	CAGGGAGTTGACCTTCATACGTT
CYP3A7	GATCTCATCCCAAACTTGGCCG	CATAGGCTGTTGACAGTCATAAATA
CYP3A43	TGGATCTCATTCCAAACTTTGCCA	GGCTGTTGCCCCTCATACAGC

[a] Annealing temperature for all primers was 62ºC

Table 3. Genotyping assay conditions for *CYP3A5* and *CYP3A7* allelic variants.

Allele	Primers (5' to 3') F = forward R= reverse		Annealing Temp (°C)	Restriction enzyme	RFLP wt pattern (bp)	RFLP variant pattern (bp)
*3A5*2*	F	CCT ACC TAT GAT GCC GTG G	56	*Dde*I	105+66+33	138+66
	R	AGT ACT TTG GGT CAT GGT GAA GAG C**cT AA**				
*3A5*3*	F	CAT GAC TTA GTA GAC AGA TGA C	55	*Ssp*I	148+125+20	168+125
	R	GGT CCA AAC AGG GAA GA**a ATA**				
*3A5*4*	F	TCG ACT CTC TCA ACA ATC C**tC**	55	*Taq*I	261+20	241+20+20
	R	AAA GTG TGT GAG GGC TC**T cGA**				
*3A5*5*	F	CCA TGA AGA TCA CCA CAA CT	53	*Nla*III	226+14	189+37+14
	R	CCT GTC CCC AGA TT**C ATg** C				
*3A5*6*	F	CAA CAA TCC ACA AGA CCC CTT TGT GGA GAG C**ct TAA**	58	*Afl*II	273+31	304
	R	GGC AGT GGG GTT TGT GGT GGG GTG				
*3A5*7*	F	CTT GAA TAT CTC CTA CAT T**Ct TAA g**TC C	60	*Afl*II	236+20	207+20+29
	R	CTC CAT CTG TAC CAC GGC ATC ATA **ctT A**				
3A5 8152 bp template	F	GAT TTA CCT GCC TTC AAT TTT TCA CTG ACC	70	--	--	--
	R	GGC AGT GGG GTT TGT GGT GGG GTG				
*3A7*1C*	F	ATG ACC TAA GAA GAT GGA GTG	55	*Ssp*I	1617+585+266	2202+266
	R	GAA GGG CAT GGT CTA CAC TAT				

Table 4: Summary of results for all phenotypic measures of CYP3A7 expression in human fetal liver.

All Samples:

	mRNA (transcripts/ng total RNA)[a]	**Protein**[b] (pmol/mg)	**T6βH**[c] (pmol/min/mg)	**T2αH**[d] (pmol/min/mg)	**DHEA16αH**[e] (nmol/min/mg)
Mean	14200	234.8	186.6	323.1	7.295
SD	15000	123.1	105.5	171.1	3.613
Median	11600	255.9	185.1	332.0	7.587
Max	95700	439.9	439.4	642.9	14.912
Min	151	0.0	2.6	3.6	0.059
Fold Range	634	-	167.1	177.4	251.1

Samples with Low Expression Excluded:

	mRNA (transcripts/ng total RNA)[1]	**Protein**[b] (pmol/mg)	**T6βH**[c] (pmol/min/mg)	**T2αH**[d] (pmol/min/mg)	**DHEA16αH**[e] (nmol/min/mg)
Mean	15503	257.6	206.3	357.7	8.071
SD	15147	106.8	91.2	141.8	2.869
Median	12529	270.2	197.9	375.0	7.884
Max	95700	439.9	439.4	642.9	14.912
Min	1326	29.0	48.4	96.6	2.412
Fold Range	72	15.2	9.1	6.7	6.2

[a] Corrected for 18S ribosomal RNA

[b] Immunoreactive CYP3A7/4 protein.

[c] Testosterone 6β-hydroxylation

[d] Testosterone 2α-hydroxylation

[e] Dehydroepiandrosterone 16α-hydroxylation

Table 5. Activities of heterologously expressed CYP3A4, CYP3A5 and CYP3A7 towards *in vitro* phenotyping probes [a]

	Testosterone Metabolite Formation (pmol/min/pmol CYP)			T2αH/T6βH Ratio	DHEA 16α Hydroxylase
CYP3A Isoform	6β-OH	2α-OH	2β-OH		(pmol/min/pmol)
rCYP3A4 [b]	46.82 ± 0.08	0.32 ± 0.01	4.60 ± 0.28	0.007	10.6 ± 0.6
rCYP3A5	1.70 ± 0.01	0.13 ± 0.01	0.22 ± 0.01	0.079	0.1 ± 0.02
rCYP3A7 [b]	0.68 ± 0.06	0.80 ± 0.06	0.21 ± 0.01	1.186	13.8 ± 1.5

[a] substrate concentrations can be found in the text

[b] CYP3A4 and CYP3A7 are co-expressed with cytochrome b_5 and oxidoreductase whereas CYP3A5 is co-expressed with oxidoreductase only. Each experimental condition was conducted in triplicate, and the data presented are the mean (± SD) of two individual experiments. Ratios of testosterone 2α-hydroxylase to 6β-hydroxylase activities (T2αH/T6βH ratios) >1.2 imply that CYP3A7 is the predominant CYP3A isoform present.

JPET Fast Forward. Published on April 21, 2005 as DOI: 10.1124/jpet.105.086504
This article has not been copyedited and formatted. The final version may differ from this version.

Figure 1

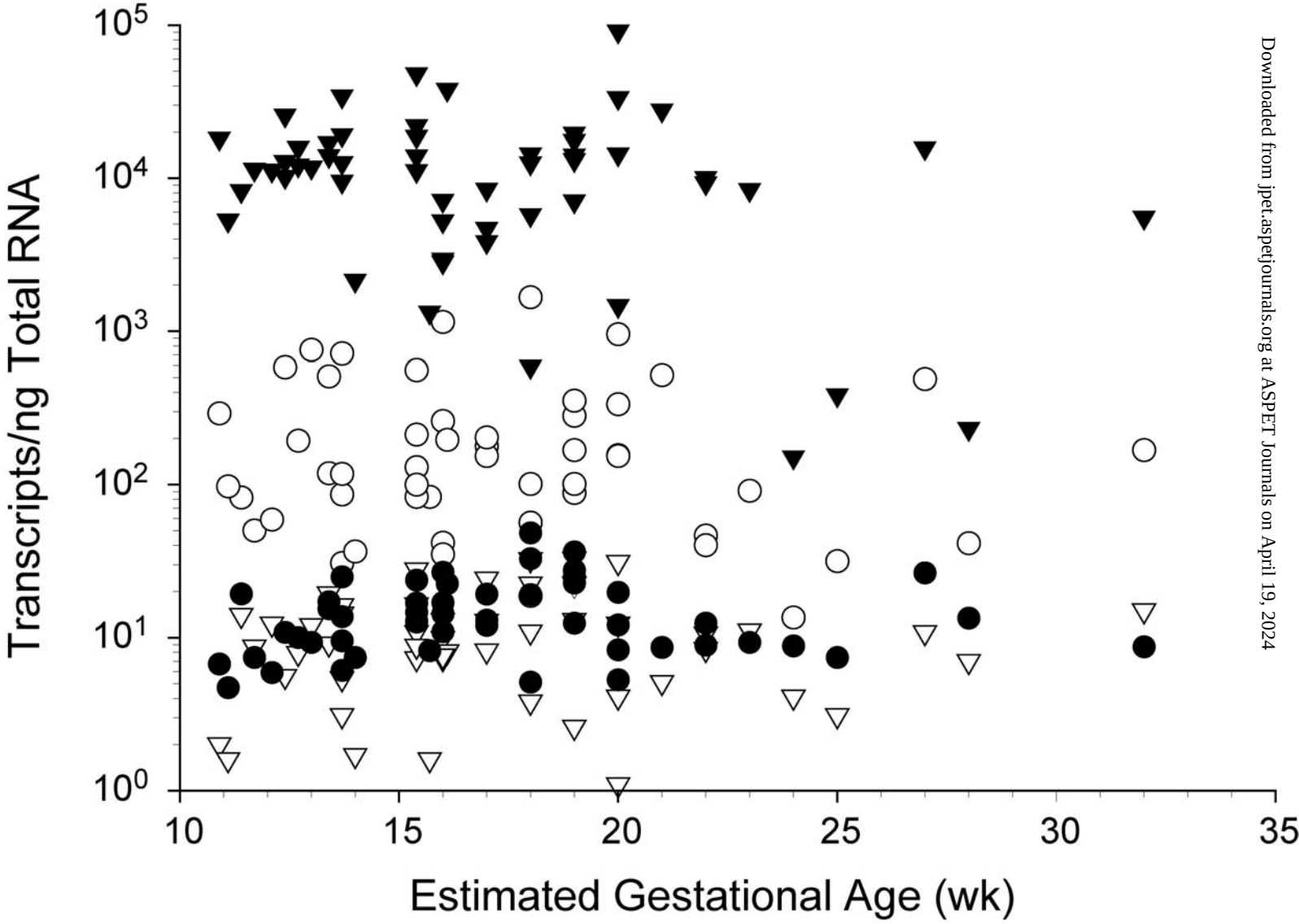

Figure 2

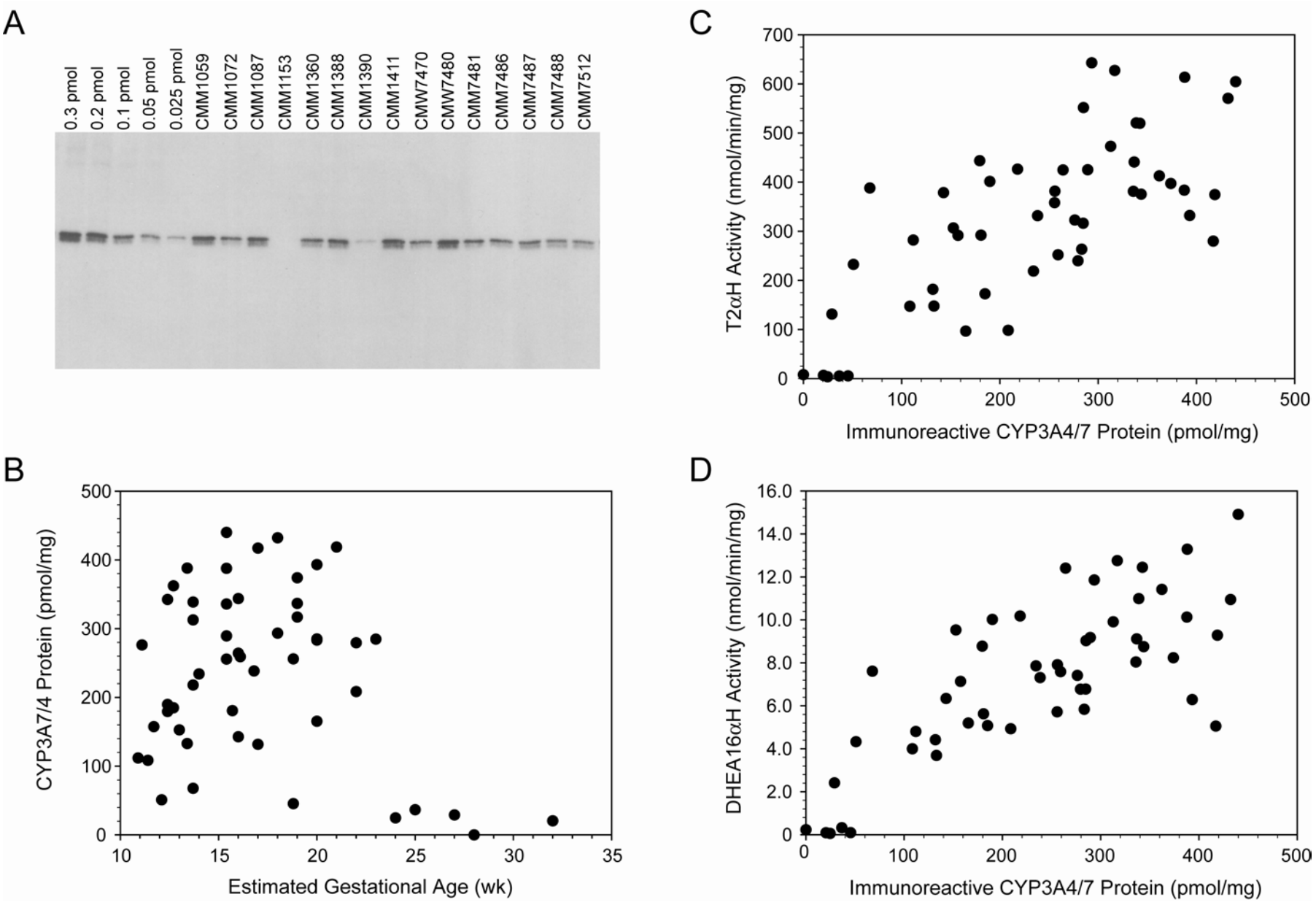

JPET Fast Forward. Published on April 21, 2005 as DOI: 10.1124/jpet.105.086504
This article has not been copyedited and formatted. The final version may differ from this version.

Figure 3

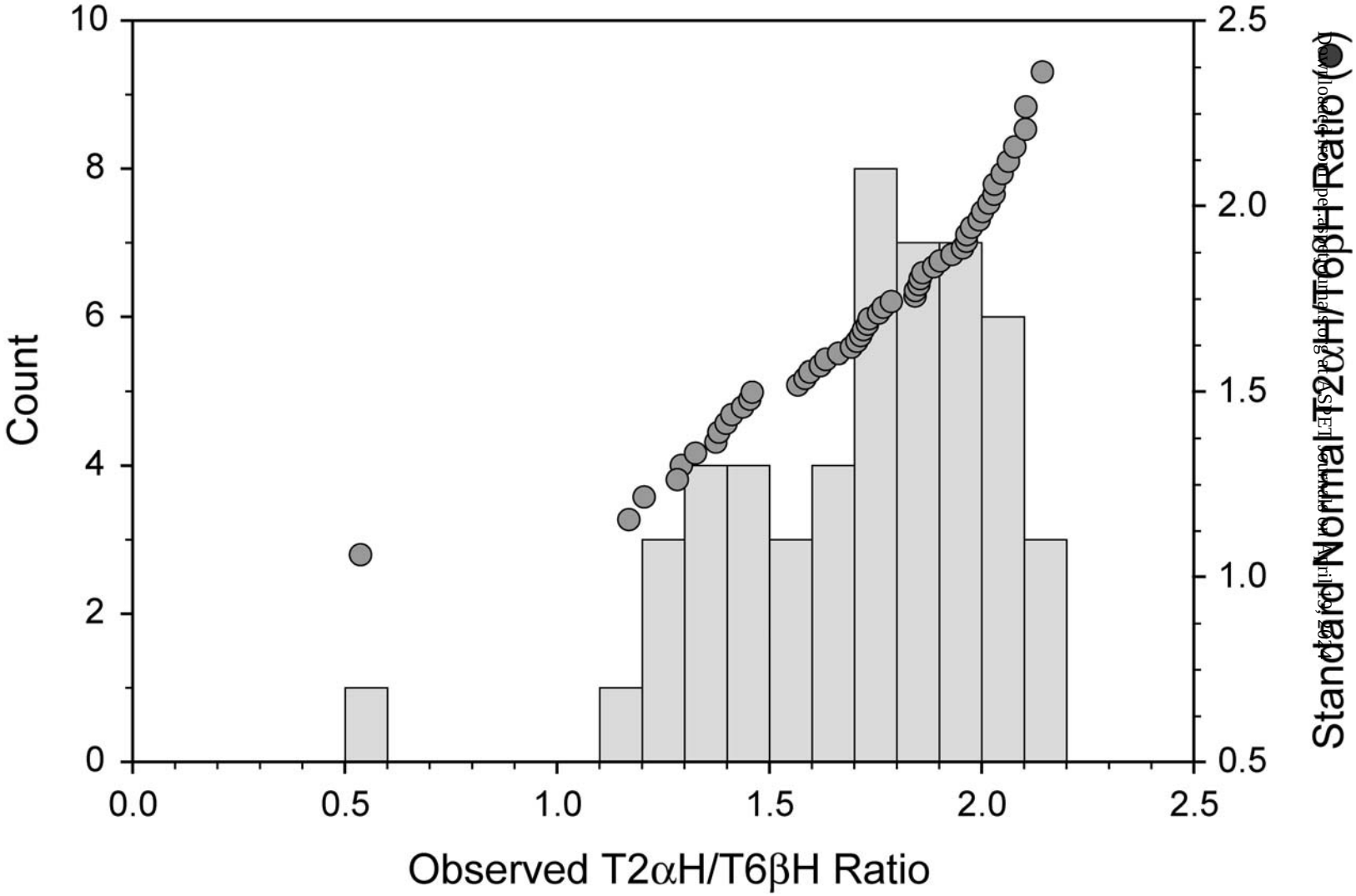

Figure 4

JPET Fast Forward. Published on April 21, 2005 as DOI: 10.1124/jpet.105.086504
This article has not been copyedited and formatted. The final version may differ from this version.

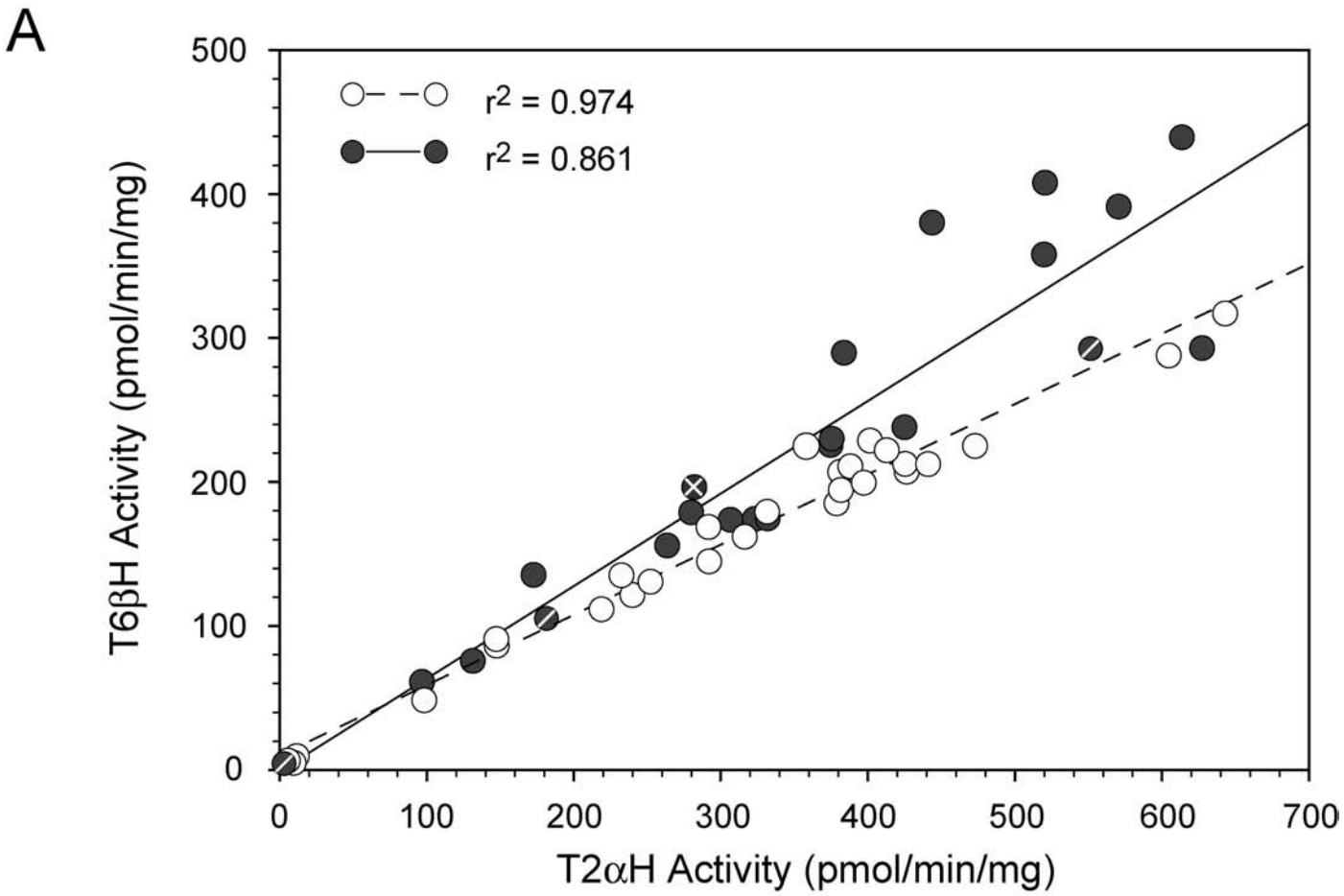

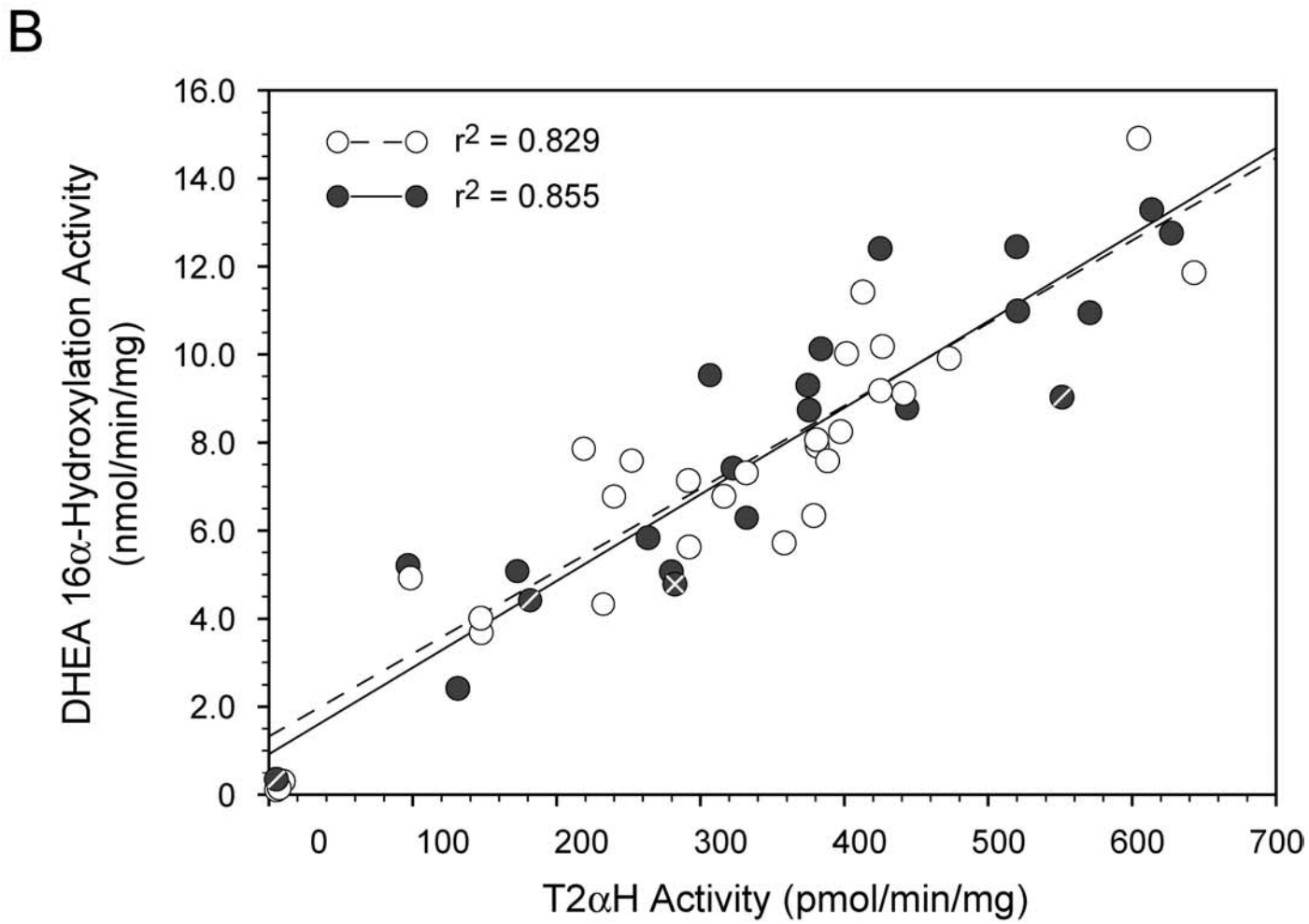

JPET Fast Forward. Published on April 21, 2005 as DOI: 10.1124/jpet.105.086504
This article has not been copyedited and formatted. The final version may differ from this version.

Figure 5